An Innovative Stimulation Technology for Permeability Enhancement in Enhanced Geothermal System — Fully Coupled Thermo-Poroelastic Numerical Approach

Nima Gholizadeh Doonechaly[1], Sheik S. Rahman[1], and Andrei Kotousov[2]

[1]School of Petroleum Engineering, University of New South Wales, Sydney
[2]School of Mechanical Engineering, University of Adelaide, Australia

Keywords

Geothermal reservoir development, roughness induced shear displacement, hydraulic stimulation, thermal stress induced permeability enhancement, fluid flow simulation in discrete fracture networks

ABSTRACT

This paper presents a new technique for stimulation of enhanced geothermal systems utilising roughness induced opening of fractures in the presence of compressive and shear stresses as well as fluid pressure inside the fracture. The thermal model is based on conductive heat transfer within the reservoir rock, convective (including conduction) heat transfer in arbitarily oriented discrete frectures and time dependent thermal equilibrium between the rock and fluid. The roughness induced shear displacement model in a thermo-poroelastic environment combined with an advanced computational technique has allowed us to simulate the opening of fractures and changes in the permeability in a geothermal reservoir. The technique was applied to a section of Soultz geothermal reservoir at a depth of 3650m and a number of numerical experiments were conducted to evaluate its geothermal potential.

Results of this study show that the average residual (retained) aperture is much lower and the time required for maximum number of observed shear dilation events due to stimulation was greater than those predicted by earlier studies including authors own study. This is due to the fact that in all these studies the surface roughness was ignored and best guess approach is used in the calculation of shear displacement. These results confirmed that the reservoir volume (contactable rock matrix by the circulating fluid) created by stimulation is much lower than the initial estimation at Soultz and Cooper Basin geothermal test sites. Results of this study also demonstrate that the effective tensile normal stresses from the injected cold fluid tend to increase fracture apertures, and hence, increase the fracture permeability within the zone of cooling. This increase in permeability is evident predominantly near wellbore region in the early circulation period. Over longer term, a significant part of the reservoir, through wich circulation is well estalished, is subjected to larger thermal stresses. These thermal stresses consequently increase permeability of the fractured network, leading to significant changes in the pressure distribution (decrease in impedance) and hence, an increase in the flow rates.

Introduction

A significant proportion of world's geothermal systems in particular Australian geothermal reservoirs are characterised by high *in situ* stresses, poorly interconnected fracture systems (Enhanced Geothermal System, EGS), steep thermal gradients and lack of aquifer support for natural recharge (Narayan et al., 1998). These conditions lead to naturally high impedance between injector and producer wells, thus making them commercially unviable. In order to overcome fluid flow barrier, a combination of hydraulic, thermal and chemical stimulation has to be employed to open, extend and interconnect the pre-existing natural network of fractures to enhance fracture conductivity.

Stimulation techniques, which are commonly employed to increase transmissivity between injection and production wells, include gel-proppant fracs, high-pressure low-injection-rate water fracs (to induce shear dilation) or a combination of both (Shaik and Rahman et al., 2009; Raymond et al., 2010; Zimmermann et al., 2010).

Gel-proppant fracs are utilised in sparsely populated, low-permeable naturally fractured reservoirs to connect the wellbore to the fracture system. *In water fracs,* the stimulation of pre-existing fractures is performed at pressures sufficiently high to cause shear failure. It has been demonstrated that under an appropriate stimulation schedule, natural fractures can slip and dilate to facilitate flow conduits in roughness-induced openings. In such a regime, upon the cessation of injection the flow conduits remain open due to the frictional resistance of rough natural fracture surfaces (Chen and Rahman et al., 2000). Typically, to initiate shear failure of natural fractures, the maximum bottom-hole injection pressure is kept in excess of the minimum formation stress at the injection point (Rahman et al., 2002; Tester et al., 2006). In order to improve the permeability of the fracture system significantly, numerous attempts have been made to maintain injection pressure at a much higher level than the minimum formation pressure. However,

there are two primary negative effects associated with increasing the throughput in such a manner: (1) fractures at higher pressures can be 'jacked' open, allowing a few paths to dominate and short circuits to occur, and (2) exceeding the critical pressure beyond which fracture growth occurs can cause the reservoir to extend beyond the circulation region, enabling water to be lost, thus reducing the effective heat-transfer area (Brown 1988; Tester et al. 2006). Such effects have been reported numerous occasions during development of geothermal sites, such as Fenton Hill, Soultz and the Cooper Basin (Tester et al., 2006).

In recent numerical studies Koh and Rahman et al (2011) observed that for a given injection pressure, *in situ* rock properties and stress conditions, the average change in aperture (shear dilation) is a function of time. According to this study, there exists a threshold time below which the change in average aperture is insignificant. After this time, the average aperture increases rapidly (until it reaches a plateau). This leads to a very important conclusion that for every set of reservoir parameters, stress condition and injection schedule, an optimum level of shear dilation can be achieved. Increase in average fracture aperture is found to be directly related to the orientation of fractures in relation to the stress field (Shaik and Rahman et al., 2009 and 2010). A subsequent thermo-poroelastic reservoir study has shown that the long-term circulation of low temperature water has a significant bearing on reservoir permeability. Thermal contraction due to cooling reduces the effective stresses (normal to the fracture surfaces) around fractures, causing an increase in aperture, but it is noteworthy that fluid-induced stress (poroelastic effect) dominates at early injection times while thermally induced stress dominates at late injection times (Koh and Rahman et al. 2010; Shaik and Rahman et al., 2011). Similar results were observed by Ghassemi et al. (2011) for a thermo-poroelastic reservoir model featuring a single co-planar fracture.

Field observations and numerical studies have shown that permeability enhancement by induced fluid pressure can be maximised by careful selection of a set of parameters that includes injection time, injected volume, and injection schedule within given operational constraints (pump rating, pressure capacities for surface facilities and so on (Rahman et al., 2002; Kohl and Rahman et al. 2007; Wang et al., 2011)). In order to achieve this objective the key processes involved in naturally fractured geothermal reservoirs must be fully integrated. Many authors have modelled these key processes in a loose or decoupled form (Jing et al., 2000; Watanabe et al., 2005 and 2010), Hossain and Rahman et al (2000) and Ghassemi (2011). Alternatively, some authors have presented coupled formulation of the abovementioned problem, but on a small local scale or with simplified fracture geometry (Ghassemi et al., 2008).

Although numerous studies have made remarkable contributions to our knowledge and provided a framework for future research, current approaches have a number of drawbacks, as discussed in a number of review papers (Rahman et al. 2002; Shaik and Rahamn et al., 2009). These techniques are largely based on simplified empirical relationships, including relationships used to calculate compressive normal surface traction, residual aperture and shear displacement, which in some cases are derived from a simple fracture experiment or a best guess. This introduces ambiguity into the simulation results and often leads to erroneous predictions of EGS behaviour.

A geological body with natural fractures, which represents the geothermal reservoir, has several distinguished length scales, like fracture aperture scale, (micro-scale) and macro-fracture scales, and inter-well scale. Despite the long history of the solid-body mechanics and recent advances in fracture mechanics, the closed system of constitutive equations describing well stimulation processes involving fracture opening and shear displacement in thermo-poroelastic media, such as geothermal systems, is not available. Constitutive models derived by Bandis et al. (1983) and Barton et al. (1985) and later extended by Willis-Richards et al. (1996) have been used extensively by authors in the prediction of shear stress-displacement behaviour at any stress level of interest, e.g. bottom-hole conditions (Rahman et al., 2002; Shaik and Rahman, et al. 2009) and (Ghassemi et al., 2011). However, geomechanical and geometrical functions used in these models are based on simple laboratory tests (not at bottom-hole conditions) and field observations as well as best-guess estimates. In a recent study by Kotousov and Rahman et al., 2011 an analytical model based on the distributed dislocation technique is used to simulate the roughness induced openings in a more realistic framework which includes a non-uniform stress distribution along the crack surface in the presence of compressive and shear stresses as well as hydraulic variant fluid pressure applied inside the fracture. This analytical model combined with advanced computational techniques is capable to accurately simulate the change in fracture geometry and provide a more realistic assessment of the permeability changes due to a hydraulic stimulation. A semi-analytical approach to the modelling of the stimulated fracture network is computationally efficient. In contrast, the computational requirement for direct discrete fracture network modelling is extremely exhaustive in the existing numerical approaches.

In this paper an innovative stimulation technology, which exploits the various fracture opening mechanisms and incorporate their possible synergistic effects to substantially in-

Table 1. Characteristics of statistical fracture sets obtained from Gentier et al. (2010). Plane direction is measured positive clockwise from North and dip positive downward from horizontal.

Fracture set #	Plane direction			Dip				Number of fractures centers/m^3	Radius [m]	Transmissivity [m^2/s]
	Distribution law used	Mean	Half-width	Distribution law used	Mean	Half-width	Dip direction			
F1	Normal	2	16	Normal	70	7	NW	$1.30\ 10^{-7}$	187	$6.0\ 10^{-6}$
F2	Normal	162	19	Normal	70	7	NE	$3.00\ 10^{-9}$	150	$6.0\ 10^{-6}$
F3	Normal	42	6	Normal	74	3	NW	$1.76\ 10^{-8}$	95	$4.0\ 10^{-6}$
F4	Normal	129	6	Normal	68	3	SW	$3.30\ 10^{-8}$	112	$2.0\ 10^{-6}$
F5	Uniform	0	180	Normal	70	9	--	$1.00\ 10^{-8}$	100	$5.0\ 10^{-7}$

crease the permeability of EGSs and improve hot water production efficiency, is presented.

Model Setup

A schematic representation of the model used in this study is shown in Fig.1. A square region of the Soultz geothermal reservoir is chosen with a side length of 1km at a depth of 3650m. Two wells, injection and production are placed at a distance of 700m apart. The reservoir is divided into 32000 grid blocks. Maximum and minimum horizontal principal stresses are acting along the x and y axis as shown in the Fig.1. Also the reservoir parameters used for this study is shown in Table 2. The abovementioned model is meshed using triangular elements. For improving the stability linear triangles are used for pressure and temperature and quadratic triangular element for the displacement degrees of freedom. No flow boundary condition is applied at the boundary of the reservoir and the fluid is injected at the injection well. The production well starts producing with a set pressure at the end of stimulation period.

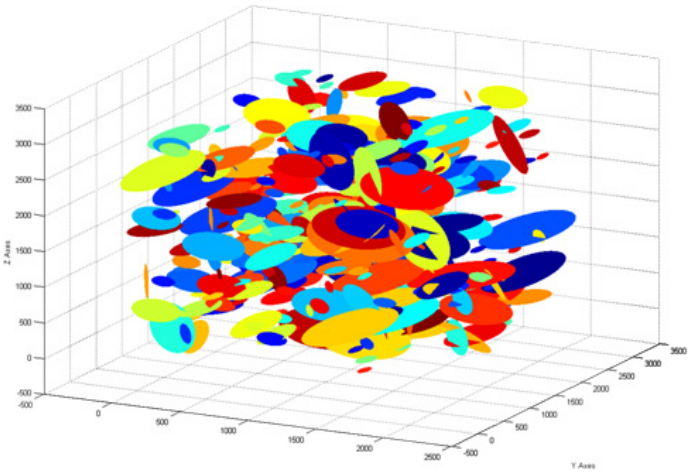

Figure 1a. Generated fracture network of the deep Soultz geothermal reservoir based on statistical data generated by Gentier et al. (2010).

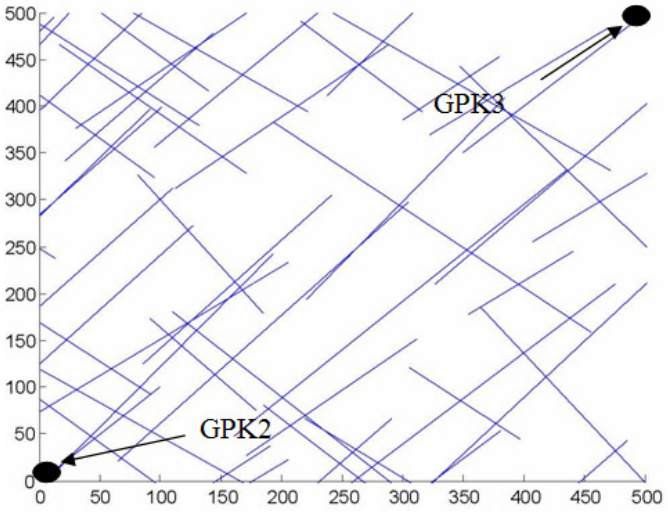

Figure 1b. A Soultz natural fracture network trace between wells GPK2 and GPK3 (open hole) at 3650 m. Trace plotted for fractures with radius greater than 60 m.

Table 2. Stress and reservoir data for strike-slip stress regime at Soulz geothermal reservoir.

Rock Properties	
Young's modulus (GPa)	40
Poisson's ratio	0.25
Density (kg/m^3)	2700
Fracture basic friction angle (deg)	40
Shear dilation angle (deg)	2.8
90% closure stress (MPa)	20
In situ mean permeability (m^2)	9.0 x 10^{-17}
Fracture Properties	
Fractal Dimension, D	1.2
Fracture density (m^2/m^3)	0.12
Smallest fracture radius (m)	15
Largest fracture radius (m)	250
Stress Data	
Maximum horizontal stress (MPa)	53.3
Minimum horizontal stress (MPa)	78.9
Fluid Properties	
Density (kg/m^3)	1000
Viscosity (Pa s)	3 x 10^{-4}
Hydrostatic fluid pressure (MPa)	34.5
Injector pressure, stimulation (MPa)	68.9
Injector pressure, production (MPa)	44.8
Producer pressure, stimulation (MPa)	N/A
Producer pressure, production (MPa)	31.0
Other Reservoir Data	
Well radius (m)	0.1
Number of injection wells	1
Number of production wells	2
Reservoir depth (m)	4430

Overall, four major computational parts are involved in this study. A fracture network is generated based on hybrid tectono-stochastic method. Then the permeability tensor is calculated for each block of the reservoir using the cubic law. Then a thermo-poro elastic finite element based model is used to characterize the induced stresses during the stimulation and production periods. After obtaining the in-situ stress distribution, the change in fracture aperture is calculated using the proposed methodology. Each of these steps is discussed below.

Discrete Fracture Network Simulation

A hybrid tectono-stochastic simulation technique is used to model the discrete fracture network of the reservoir (Gholizadeh Doonechaly and Rahman, 2012). In this study, statistical data on fracture properties and reservoir structure of the Soultz available in the open literature are used to construct the fracture map (Gemtier et al, 2010, see Table1). For the purpose of in-situ stress history modeling a Finite Element Method (FEM) is used to reconstruct the reservoir structure by unfolding and folding (reverse and forward model) in a single tectonic event. Also a non-linear visco-elastic model is used to consider the effect of deformation on rock viscosity. After reconstructing the original shape of the layer, stress tensor values as well as the stress invariants are calculated for each node based on the deformation history of the model. Mohr-

Colomb fracture criterion, which relates the critical strength of the material to its stress state, is used to determine whether the obtained stress exceeds strength (shear) of the rock. If the obtained stress tensor satisfies failure criterion, stress invariants are used to calculate the rate of formation of fractures for each node. Rate of formation of fractures is used as one of the most important input parameters for the next step of the Neural-stochastic simulation. As part of neuro-stochastic simulation, fracture properties (fracture density and fractal dimension) are generated based on their characterized statistical distribution obtained from tectonic simulation and field data (as listed in Table 1). In the next step the reservoir is divided into a number of grid blocks. Fracture density and fractal dimension are estimated for the blocks where the fracture data are available. Then the neural network is used to develop a 3D continuum map of fracture density and fractal dimension. Finally, the sequential Gaussian stochastic simulation combined with simulated annealing technique is used to generate the discrete fracture network. The 3D discrete Fracture map of Soultz reservoir as well as its 2D map at depth of 3650m are presented in Figs.1 and 2 respectively.

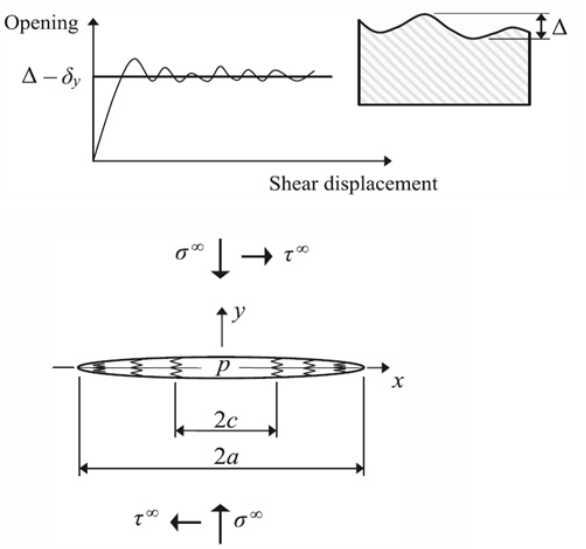

Figure 2. Opening versus shear displacement (top) and roughness induced fracture opening (bottom).

Fluid Flow Simulation

For the fluid flow simulation the permeability tensor of each grid block is made known as a priori. In this study, the effective permeability tensors as proposed by Teimoori and Rahman et al (2003) and later modified by Fahad and Rahman (2011) is estimated for each grid block. In this methodology, short fractures are considered as part of the matrix pores and the fluid flow through them is simulated using the Darcy's law and Laplace equation. Also the boundaries of the short fractures are subjected to the interface boundary condition. Flow in the medium to long fractures is characterized by the Cubic law. Flow region between matrix and fracture is characterized as Poisson's region and fluid flow in this region is modeled after Teimoori and Rahman, et al (2005). The effective permeability tensor is used in the next step as part of the thermo-poroelastic model of the reservoir.

Thermo-Poroelastic Model

A finite element based thermo-poroelastic model is developed for evaluating fluid flow, pressure and temperature at different sections of the reservoir. Development of such a model consists of three parts: a) deformation of the porous media within the reservoir caused by the in-situ stresses and injection pressure, b) fluid flow within the reservoir, and thermal conduction and convection by diffusion and advection respectively. The governing equations used for the fully coupled thermo-poroelasticity are as follows: (Kurashige, 1989; Ghassemi et al., 2002 ; Shaik and Rahman, 2011):

$$\left(K+\frac{G}{3}\right)\nabla(\nabla\cdot u)+G\nabla^2 u-\alpha\nabla p-\gamma_1\nabla T_R=0$$

$$\frac{\partial\zeta}{\partial t}=\frac{k}{\mu}\nabla^2 p \tag{1}$$

$$\dot{\zeta}=\alpha\dot{\varepsilon}_{ii}+Q'\dot{p}-\gamma_2\dot{T} \tag{2}$$

$$\dot{T}_f+\nabla(J_f T_f)-c_f^T\nabla^2 T_f=0 \tag{3}$$

$$\dot{T}_R-c_R^T\nabla^2 T_R=0 \tag{4}$$

Where, K is the bulk modulus , G is the shear modulus , u is the displacement, α is the Biot's coefficient, γ_1 is the thermal expansion coefficient of solid, γ_2 is the thermal expansion coefficient of fluid (K^{-1}), T_R is the rock temperature, T_f is the fluid temperatures and p is the pore pressure. The above governing equations have allowed us to formulate instantaneous non-equilibrium heat transfer between fluid in fracture and matrix which results in stress perturbation.

Fracture Response to Stimulation Model

The analytical model recently developed by Kotousov and Rahman, et al 2011 is used to model the shear slippage of the fracture surfaces with respect to each other which causes the change in the fracture aperture. Two main assumptions are made for this purpose. Firstly, the sliding of the fracture surfaces with respect to each other is characterized using the classical Coulomb friction law as:

$$\tau_n=\tau_0+f\sigma_n \tag{5}$$

Where, τ_0 is the threshold shear stress at which the fracture surfaces start to slide, f is the friction factor, σ_n is the normal stress and τ_n is the shear stress during the slippage.

Next, the fracture aperture is described based on the surrounding in-situ stress condition. In this model any shear displacement of the surfaces of the fracture causes the fracture to open. The effect of the roughness of the fracture faces is simulated by distributed elastic springs as illustrated in Fig.2. The contact between surfaces diminishes when the opening exceeds the overall the roughness of the fracture surfaces. The constitutive equations for the adopted simplified model are as follow:

$$\sigma_n=k\bar{E}(\Delta-\delta_y)\qquad \delta_y<\Delta \tag{6}$$

$$\sigma_n = 0 \qquad \delta_y \geq \Delta \tag{7}$$

As shown in Fig. 3 the force is assumed to be zero at the places where there is no contact between the fracture surfaces. This phenomenon is characterized by a value named characteristic height of the fracture, Δ. Also E is the Young modulus of elasticity and k is the spring constant. Based on the above assumptions, the boundary value problem describing the shear displacement of fracture surfaces can be formulated as follow:

$$\sigma_{yy} = \sigma^{\infty} \qquad x^2 + y^2 \to \infty \tag{8}$$

$$\sigma_{yy} = k\bar{E}(\Delta - \delta(x)) + p \qquad c < |x| \leq a \tag{9}$$

$$\sigma_{yy} = p \qquad c \geq |x| \tag{10}$$

$$u_y = 0 \qquad |x| > a \tag{11}$$

$$\tau_{xy} = \tau^{\infty} \qquad x^2 + y^2 \to \infty \tag{12}$$

$$\tau_{xy} = \tau_0 + f\sigma_n = \tau_0 + f(k\bar{E}(\Delta - \delta(x)) + p) \tag{13}$$

As can be seen from the above equations, the solution for mode I fracture propagation can be obtained first since it will affect the solution of the mode II fracture. By using the dislocation densities as proposed by Codrington and Kotousov (2007a and b), the stress distribution around the fracture can be calculated. Finally, it will result in a system of linear equations (see Kotousov and Rahman, 2011 for details):

$$\frac{1}{N}\sum_{i=1}^{N}\frac{\phi_y(S_i)}{t_j - S_i} = \frac{4}{\bar{E}}(-\sigma^{\infty} - p) \qquad \delta(t_j) \geq \Delta \tag{14}$$

$$\frac{1}{N}\sum_{i=1}^{N}\frac{\phi_y(S_i)}{t_j - S_i} = -\frac{4}{\bar{E}}(-\sigma^{\infty} + p + k\bar{E}\Delta)$$

$$+4\pi\frac{ka}{N}\sum_{i=1}^{i<j}\phi_y(S_i) \qquad \delta(t_j) < \Delta \tag{15}$$

Where, Eq. (15) is to be set for each characteristic point of the fracture surface (j). Also ϕ is the function related to the dislocation density as comprehensively discussed in (Kotousov, 2007). The solution of this system of equations is obtained by solving the system of linear equations. The fracture opening caused by the shear displacement at each point of the reservoir is calculated based on the following formula:

$$\delta(t_j) = \frac{1}{N}\sum_{i=1}^{i<j}\phi_y(S_i) \tag{16}$$

The updated fracture aperture is implemented in the next simulation time step to analyze the behavior of the network of fractures.

Results and Discussion

Initially, field data, such as the reservoir structure, fracture orientation, size and other fracture parameters, that influence reservoir performance, from Soultz geothermal reservoir are acquired from the open literature.

An analysis of hot water production in terms of well placement is performed for two well configuration, GPK2 and GPK3 where GPK 2 is the injection well and GPK 3 the production well. Well location and distance between wells are chosen based on the Soultz EGS system. This information is used to investigate fracture stimulation by injected fluid pressure and thermal stress and consequent changes in permeability (in terms of Log_{10} RMS fluid velocity) both in short and long term. The reservoir permeability for each block is calculated based on the discrete fracture network data and fluid flow simulation. Then the injector, GPK2 is pressurised and the pore pressure, Log_{10} RMS velocity, temperature and stress tensor across the reservoir at each time step are estimated. Residual fracture aperture as a result of change in local stress, pore pressure and temperature are determined and evaluated. Results of stress and pore pressure are used to calculate current total aperture (accounting for the fracture opening (mode I), shear dilation (mode II)) for each individual natural fracture and update the permeability of the reservoir.

In the current thermo-poroelastic numerical model, flow between the injection and production wells are assumed to be planar and is approximated through the open hole interval (3500m to 3800m) through a statistically representative trace. The well placements on the plane are taken as their separation at a depth of 3650m, which is midway through their depth-averaged open hole sections. The reservoir is pressurized by injecting fluid through the injection well (GPK2). To increase the injectivity, a pair of co-planar fractures of half-length of 50m is placed at both the injection and production wells. The pressurization was carried out over a period of 52 weeks. During the pressurization, the change in fracture width for each individual natural fracture and the resulting permeability tensor were calculated. Following stimulation of the reservoir, a flow test was carried out over a period of 14 years. During the flow test, changes in fracture apertures due to thermo-poro-elastic stresses and the consequent changes in permeability were determined. Also estimated were the thermal drawdown, produced fluid temperature and production rate of the Soultz EGS.

Effect of Stimulation Time on Shear Dilation

Results of shear dilation are presented as average percentage increase in fracture aperture and dilation events with time (see Figs. 3 and 4a, b and c). From Fig. 3, it can be seen that there exists three distinct aperture histories: 0-40 weeks, 40-50 weeks

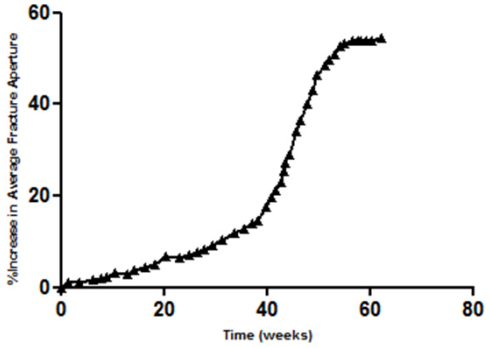

Figure 3. Increase in average fracture aperture (retainable) with stimulation time. Strike slip stress regime with σH = 51.7 MPa and σh = 44.8 MPa, P_{inj} = 51.7 MPa.

and 50 weeks and above. Until about 40 weeks, a slow but linear increase in occurrence of dilation events due to induced fluid pressure of 51.7 MPa (bottomhole) and reaches a value of about 18% (average increase in aperture). Following this time, the rate of occurrence of dilation events increases sharply until about 50 weeks, thus reaching 60% increase in average fracture aperture. After which, no significant dilation events can be observed (a plateau of events is reached). This infers that for every set of reservoir and stress parameters as well as injection schedule, an optimum level of shear dilation can be achieved. In Figs. 4 (a, b and c) the dilation events at different stimulation times are presented. From these figures it can be seen that it takes about 50 weeks for shear dilation events to reach the production well. When the results of this study are compared with previous study (Koh and Rahman et al, 2011), in which shear dilation events are estimated based on a simplistic model (Willis-Richards et al, 1996) a number of distinct features can be observed. Firstly the time required to overcome the threshold stress is 40 weeks which is about 12 weeks longer than the previous studies. Secondly, the time required to create maximum effective reservoir volume is almost 20 weeks longer than the previous studies (40 weeks). Results of this study clearly demonstrate that the material properties, such as the surface roughness and Modulus of Elasticity used to estimate residual aperture provide a more realistic prediction of shear displacement events and the resulting residual aperture. These values are obviously more conservative than that previously observed. These results confirm that the reservoir volume (interconnected fracture networks for effective the heat transfer area) estimated by the new stimulation technique (this study) is much smaller (lower retained fracture aperture) than estimated by previous studies.

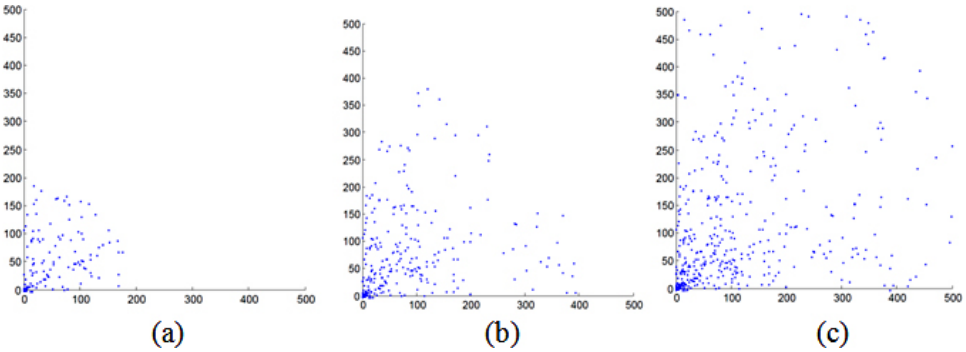

Figure 4. Cumulative shear dilation events of the fracture network during different stages of stimulation: after (a) 1 week, (b) after 24 weeks and (c) after 52 weeks for a strike slip stress regime with σH = 51.7 MPa and σh = 44.8 MPa, P_{inj} = 51.7 MPa. The event's locations are in the Cartesian coordinates in meters.

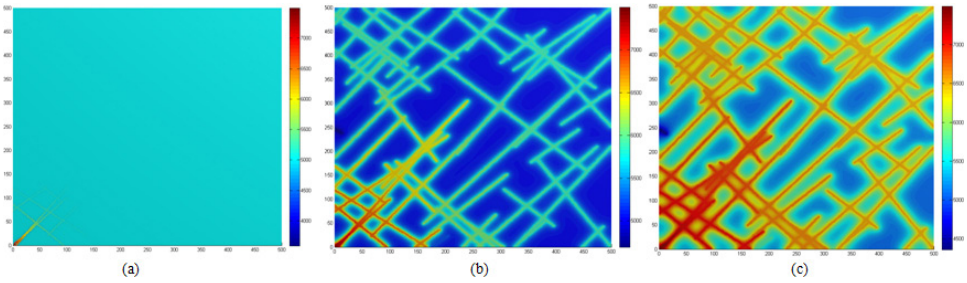

Figure 5. Pore pressure distribution of the fractured reservoir at different stimulation stages: after (a) 1 week, (b) 40 weeks and (c) 52 weeks for a strike slip stress regime with σH = 51.7 MPa and σh = 44.8 MPa, P_{inj} = 51.7 MPa.

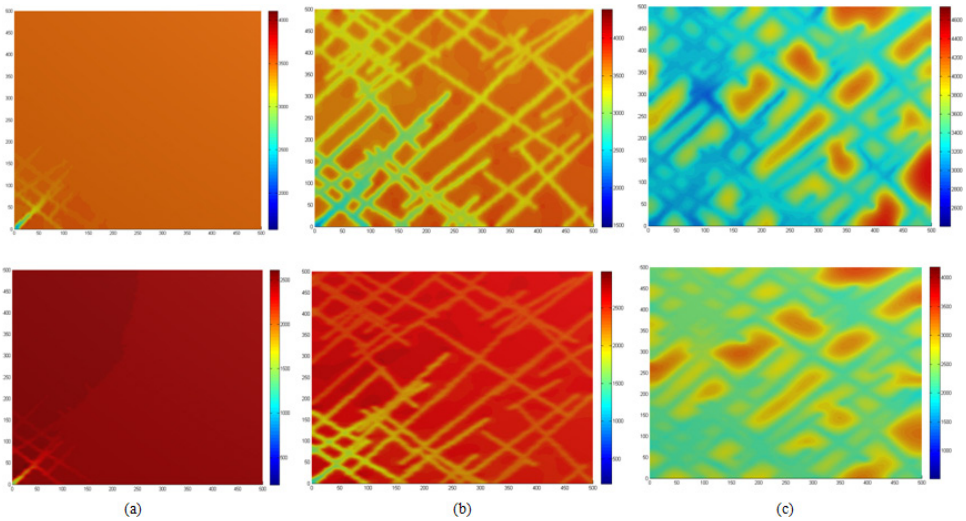

Figure 6. x (top) and y (bottom) components of effective stress distribution at different stimulation stages: after (a) 1 week, (b) 40 weeks and (c) 52 weeks for a strike slip stress regime with σH = 51.7 MPa and σh = 44.8 MPa, P_{inj} = 51.7 MPa.

In Figs. 5 (a, b and c) and 6 (a, b and c) pore pressure and effective stress (x and y components) profiles at 1 week, 40 weeks and 52 weeks of stimulation are presented respectively. From the results of pore pressure it is evident that by 40 weeks the injection pressure sweeps through almost all fractures and by 52 weeks pore pressure is well established throughout the reservoir. Similarly the effective stress (both x and y direction) throughout the reservoir is significantly reduced by 52 weeks.

Numerical Flow Test

Following the 52 weeks of stimulation, a flow test was carried out with a bottomhole injection pressure of 51.7 MPa and a production pressure of 31.7MPa (at a reservoir impedance of 20 MPa between the injection and production wells) for period of 14 years. During this production period, pore pressure profile, Log_{10} root means square (RMS) velocity profile (which is directly proportional to the permeability), effective stress and the matrix temperature drawdown are monitored. In Figs 7 (a, b, and c) and 8 (a, b, and c) the

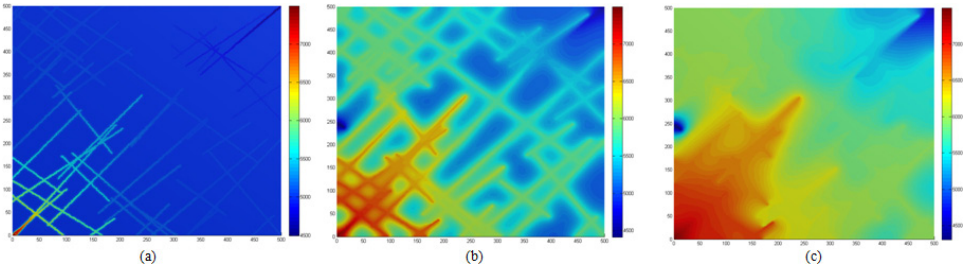

Figure 7. Pore pressure distribution at different production stages: after (a) 1 month, (b) 3 years and (c) 14 years of for σH = 51.7 MPa and σh = 44.8 MPa, P_{inj} = 51.7 MPa and P_{prod}=31.7 MPa.

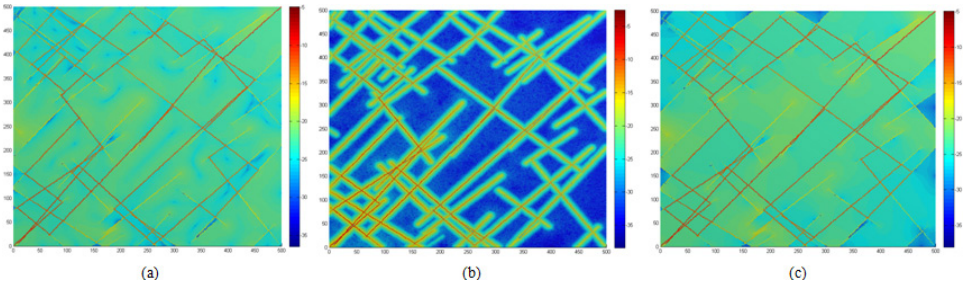

Figure 8. Log_{10} RMS velocity profile at different production stages: after (a) 1 month, (b) 3 years and (c) 14 years of production for σH = 51.7 MPa and σh = 44.8 MPa, P_{inj} = 51.7 MPa and P_{prod}=31.7 MPa.

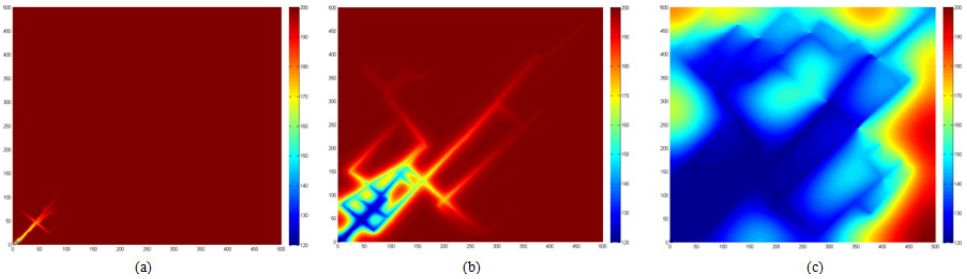

Figure 10. Rock matrix temperature distribution at different production stages: (a) 1 month, (b) 3 years and (c) 14 years for σH = 51.7 MPa and σh = 44.8 MPa, P_{inj} = 51.7 MPa and P_{prod}=31.7 MPa, T_{inj} = 120 °C, T_{matr} = 200 °C.

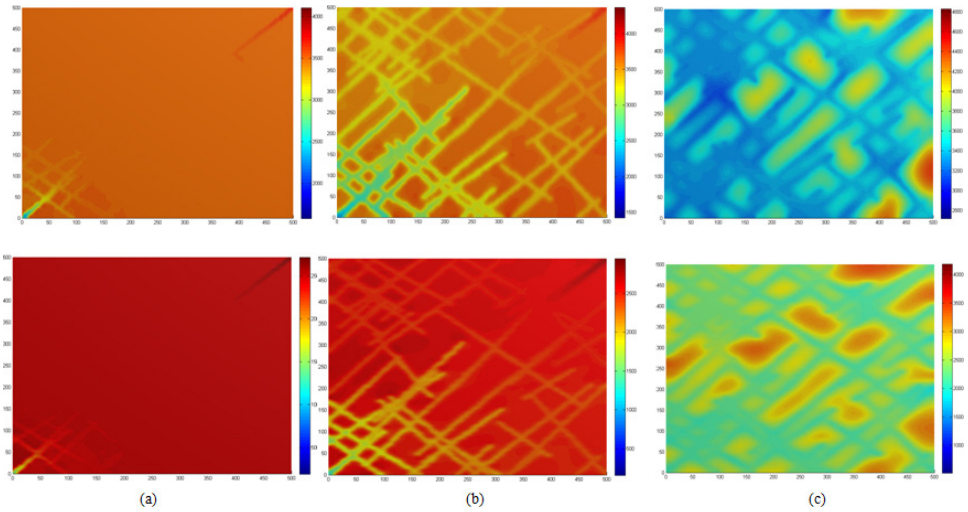

Figure 11. x (top) and y (bottom) components of effective stress distribution at different production stages: (a) 1 month, (b) 3 years and (c) 14 years for σH = 51.7 MPa and σh = 44.8 MPa, P_{inj} = 51.7 MPa and P_{prod}=31.7 MPa, T_{inj} = 120 °C, T_{matr} = 200 °C.

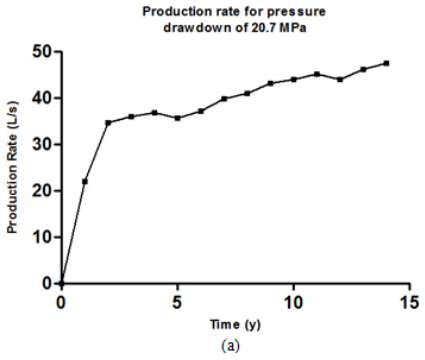

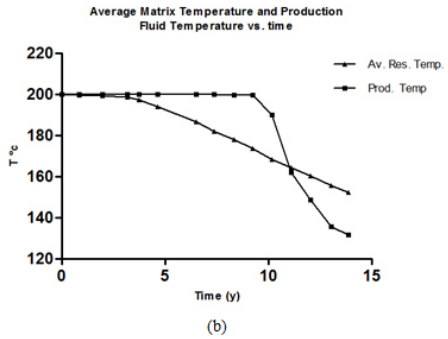

Figure 9. Average matrix temperature drawdown, produced fluid temperature (b) and production rate (a) for pressure draw down of 20MPa over a production period of 14 years after stimulation for a period of 52 weeks. σH = 51.7 MPa and σh = 44.8 MPa, P_{inj} = 51.7 MPa and P_{prod}=31.7 MPa.

pore pressure and the Log_{10} RMS fluid velocity profile after 1 month, 3 years and 14 years are presented respectively. From the results it can be observed that during the early production period (one month) high pore pressure is primarily built up around the injection well and the flow of fluid is primarily through major inter-connected flow paths (see Figs 7 a and 8 a). With the progress of time the injection pressure advances towards the production well and at the about 3 years of production time it reaches half way between the injection and production wells. By this time the fluid sweeps through a significant part of the reservoir. From production history data (as presented in Fig 9) it is evident that the production increased from 2 l/s after one month of production to 45 l/s after 14 years of production. During the same period produced fluid temperature dropped from 200 to 140 °C. Matrix temperature drawdown for the same period of production (14 years) is presented in Figs (10 a, b and c). Because of the low fluid and rock matrix contact area at the early stage of production, the heat transfer and

the resulting thermal drawdown is very low (see Fig 10 a). With the pass of time the fluid sweeps over a large part of the reservoir which increases thermal drawdown. At the end of the 14 years of production the average matrix temperature drops from 200 to 150°C which is quite low (drop) compared to previous studies (drop of 80°C over the production period of 14 years (Koh and Rahman, 2011)) under the same reservoir conditions. In Fig 11 the x- and y components of effective stress distribution of the Soultz geothermal reservoir during different stages of production are presented. These results show that by the end of 14 years of production the effective stresses throughout the reservoir are significantly reduced, thus allowing most fractures to open and conduct fluid. The reduction in the effective stresses is caused by the circulating fluid as well as thermal drawdown. In Figs. 12 and 13 the Log_{10} RMS fluid velocity and effective stresses with and without the thermal effects (poro-thermo-elastic and poro-elastic) at the end of 14 years of production are presented respectively. Results confirms that the thermal stress due to cooling of the reservoir has a significant bearing in reducing the effective stresses which in turns increases the fracture aperture and therefore the Log_{10} RMS fluid velocity (see Figs. 12 and 13).

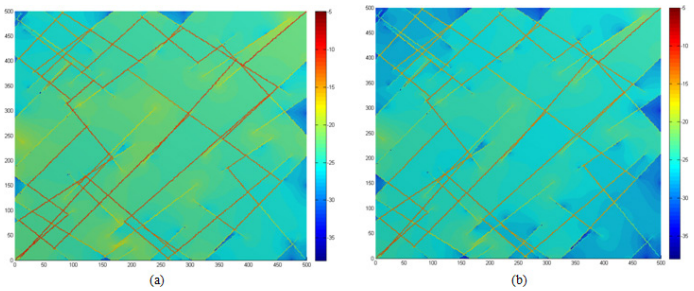

Figure 12. Log_{10} RMS velocity profile after a production period of 14 year: (a) with and (b) without considering thermal stresses for σH = 51.7 MPa and σh = 44.8 MPa, P_{inj} = 51.7 MPa and P_{prod}=31.7 MPa, T_{inj} = 120 °C, T_{matr} = 200 °C.

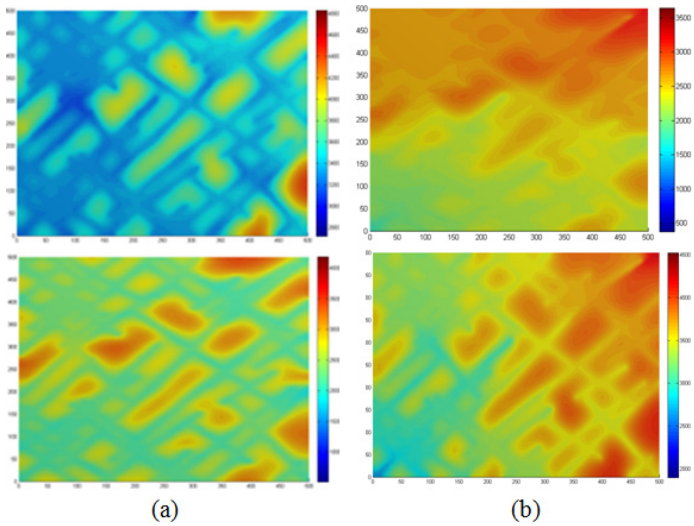

Figure 13. x (top) and y (bottom) components of effective stress distribution after 14 years of production: (a) with poro-thermo-elastic effect and (b) with poro-elastic effect for σH = 51.7 MPa and σh = 44.8 MPa, P_{inj} = 51.7 MPa and P_{prod}=31.7 MPa, T_{inj} = 120 °C, T_{matr} = 200 °C.

Conclusions

In this paper, a roughness induced shear displacement model in a poro-thermoelastic environment combined with an advanced computational technique is used to study the effects of induced fluid pressure and thermal stresses (cooling effect) on reservoir permeability and consequent increase in hot water production. Because the model is based on analytical solution it was possible to integrate the shear displacement model within the fluid flow and heat transfer model (with less computation effort) to predict stress changes due to induced fluid pressure and thermal drawdown and the resulting changes in fracture aperture. The new poro-thermoelastic model was applied to the Soultz geothermal reservoir, France and the effect of water circulation on stress changes over longer term investigated. From the results of this study, the following conclusions can be drawn.

It has been shown that surface roughness induced shear displacement provides a more realistic prediction of residual fracture aperture. These results agree well with the experience of existing EGS trials around the world. An average increase in aperture due to fluid induced shear dilation has been found to be lower and time required to obtain a maximum stimulated volume is greater. Results of this study are in consistent with that of previous studies: for every geothermal system there exists an optimum injection schedule (injection pressure and duration). Any further increases in stimulation effort, i.e. stimulation time for a given stimulation pressure, does not provide additional permeability enhancement.

Thermal stresses induced during the circulation of cold water have a significant bearing on the long term production rate. As thermal drawdown of the rock matrix takes place, tensile thermal stresses are induced which allow residing fractures to dilate and enhance permeability. This gradually increases the fluid velocities between the injector and producer, yielding increasing production rates with time.

References

Baria, R., Baumg¨artner, J., G´erard, A., Jung, R., Garnish, J., 1999. European HDR research programme at Soultz-sous-For ̂ets (France) 1987–1996. Geothermics 28, 655–669.

Beeler, N.M., Simpson, R.W., Hickman, S.H. and Lockner, D.A., 2000. Pore fluid pressure, apparent friction, and Coulomb failure, J. Geophys. Res. 105, 25533– 25542.

Beeler, N. M., Wong, T. F. & Hickman, S. H., 2003. On the expected relationships among apparent stress, static stress drop, effective shear fracture energy, and efficiency. Bull. Seismol. Soc.Am. 93, 1381-1389.

Ghassemi, A. and G. Suresh Kumar (2007). „Changes in fracture aperture and fluid pressure due to thermal stress and silica dissolution/precipitation induced by heat extraction from subsurface rocks.“ Geothermics 36(2): 115-140.

Ghassemi, A., Nygren, A., Cheng, A., 2008. Effects of heat extraction on fracture aperture:A poro–thermoelastic analysis. Geothermics 37, 525–539.

Gentier, S., Rachez, X., Ngoc, T. D. T., Peter-Borie, M. and Souque, C. (2010). „3D Flow Modelling of the Medium-Term Circulation Test Performed in the Deep Geothermal Site of Soultz-Sous-forets (France). Proceedings Worlf Geothermal Congress 2010 - Bali, Indonesia, 25-29 April 2010.

Jing, Z., J. Willis-Richards, et al. (2000). „A three-dimensional stochastic rock mechanics model of engineered geothermal systems in fractured crystalline rock.“ J. Geophys. Res. 105.

Koh, J., H. Roshan, et al. (2011). „A numerical study on the long term thermo-poroelastic effects of cold water injection into naturally fractured geothermal reservoirs.“ Computers and Geotechnics 38(5): 669-682.

Kumar, G.S. and Ghassemi, A., 2005. Numerical modeling of non-isothermal quartz dissolution/precipitation in a coupled fracture–matrix system. Geothermics 34 (2005) 411–439.

McDermott, C.I. and Kolditz, O., 2006. Geomechanical model for fracture deformation under hydraulic, mechanical and thermal loads. Hydrogeol. J. 14, 487–498.

Murphy, P. Negraru and M. Richards 2007 Impact of enhanced geothermal systems on US energy supply in the twenty-first century Journal: Philosophical Transactions of the Royal Society A: Mathematical, Physical and Engineering Sciences Volume: 365 Issue: 1853 Pages: 1057-1094 Date: April 15, 2007.

Muskat, M. (1937). The Flow of Homogeneous Fluids Through Porous Media, Edwards Publisher.

Narayan, S. P., Z. Yang, et al. (1998). HDR reservoir development by fluid induced shear dilation: A numerical study of the Soultz and the Cooper Basin granite rock. International Hot Dry Rock - Forum, Strasbourg, France.

O'Sullivan, M.J., Pruess, K., Lippmann, M.J., 2001. Geothermal reservoir simulation. The state of practice and emerging trends. Geothermics 30 (4), 395–429.

Rahman, M. K., M. M. Hossain, et al. (2000). „An analytical method for mixed-mode propagation of pressurized fractures in remotely compressed rocks.“ International Journal of Fracture 103(3): 243-258.

Rahman, M. K., M. M. Hossain, et al. (2002). „A Shear-Dilation-Based Model for Evaluation of Hydraulically Stimulated Naturally Fractured Reservoirs.“ Int. J. for Numerical and Analytical Methods in Geomech. 26(5).

Sanyal, S. K., E. E. Granados, et al. (2005). An Alternative and Modular Approach to Enhanced Geothermal Systems. World Geothermal Congress 2005, Antalya, Turkey.

Sausse, J., Desayes, C. and Genter, A. (2007). „From geological interpretation and 3D modelling to the characterization of the deep seated EGS reservoir of Soultz (France).“ Proceedings European Geothermal Congress 2007, Unterhaching, Germany, May 30-June 1, 2007.

Shaik, A. R., M. A. Aghighi, et al. (2008). "An Innovative reservoir simulator can Help Evaluate Hot Water Production for Economic Development of Australian Geothermal reservoirs." GRC Transactions 32: 97 102.

Shaik, A.R., Koh, J., Rahman, S. S., Aghighi, M. A. and Tran, N. H., 2009. Design and evaluation of well placement and hydraulic stimulation for economical heat recovery from enhanced geothermal systems. GRC Annual Meeting October 4–7, 2009, conference proceedings.

Shaik, A. R., S. S. Rahman, et al. (2011). "Numerical simulation of Fluid-Rock coupling heat transfer in naturally fractured geothermal system." Applied Thermal Engineering 31(10): 1600-1606.

Shaik, A.R., Koh, J., Rahman, S. S., Aghighi, M. A. and Tran, N. H., 2009. Design and evaluation of well placement and hydraulic stimulation for economical heat recovery from enhanced geothermal systems. systems. GRC Annual Meeting October 4–7, 2009, conference proceedings.

Tran, N., Z. Chen, et al. (2007). "Characterizing and modelling of fractured reservoirs with object-oriented global optimization." Journal of Canadian Petroleum Technology 46(3): 39-45.

J. W. Tester, B. J. Anderson, A. S. Batchelor, D. D. Blackwell, R. DiPippo, E. M. Drake, J. Garnish, B. Livesay, M. C. Moore, K. Nichols, S. Petty, M. Nafi Toksoz, R. W. Veatch, R. Baria, C. Augustine, E.

Willis-Richards, J., K. Watanabe, et al. (1996). "Progress toward a stochastic rock mechanics model of engineered geothermal systems." J. Geophys. Res. 101(B8): 17481-17496.

Zimmermann, G., Moeck, I., Blöcher, G. (2010): Cyclic waterfrac stimulation to develop an enhanced geothermal system (EGS): Conceptual design and experimental results. - Geothermics, 39, 1, 59-69.

Zhou, X. X., Ghassemi, A. and Cheng, A. H.-D., 2009. A three-dimensional integral equation model for calculating poro- and thermoelastic stresses induced by cold water injection into a geothermal reservoir. Int. J. Numer. Anal. Meth. Geomech. 2009; 33,1613–1640.